Production of Polyunsaturated Fatty Acids by Polyketide Synthases in Both Prokaryotes and Eukaryotes

James G. Metz,[1*] Paul Roessler,[2†] Daniel Facciotti,[2†] Charlene Levering,[2] Franziska Dittrich,[2] Michael Lassner,[2†] Ray Valentine,[2] Kathryn Lardizabal,[2] Frederic Domergue,[3] Akiko Yamada,[4†] Kazunaga Yazawa,[4†] Vic Knauf,[2†] John Browse[3*]

Polyunsaturated fatty acids (PUFAs) are essential membrane components in higher eukaryotes and are the precursors of many lipid-derived signaling molecules. Here, pathways for PUFA synthesis are described that do not require desaturation and elongation of saturated fatty acids. These pathways are catalyzed by polyketide synthases (PKSs) that are distinct from previously recognized PKSs in both structure and mechanism. Generation of cis double bonds probably involves position-specific isomerases; such enzymes might be useful in the production of new families of antibiotics. It is likely that PUFA synthesis in cold marine ecosystems is accomplished in part by these PKS enzymes.

PUFAs are critical components of membrane lipids in most eukaryotes (*1*, *2*) and are the precursors of certain hormones and signaling molecules (*3*, *4*). Known pathways of PUFA synthesis involve the processing of the saturated 16:0 (*5*) or 18:0 products of fatty acid synthase (FAS) by elongation and aerobic desaturation reactions (*6–8*). The synthesis of docosahexeanoic acid (DHA, 22:6ω3) from acetyl–coenzyme A (acetyl-CoA) requires approximately 30 distinct enzyme activities and nearly 70 reactions, including the four repetitive steps of the fatty acid synthesis cycle. PKSs carry out some of the same reactions as FAS (*9*, *10*) and use the same small protein (or domain), acyl carrier protein (ACP), as a covalent attachment site for the growing carbon chain. However, in these enzyme systems, the complete cycle of reduction, dehydration, and reduction seen in FAS is often abbreviated, so that a highly derivatized carbon chain is produced, typically containing many keto and hydroxy groups as well as carbon-carbon double bonds in the trans configuration. The linear products of PKSs are often cyclized to form complex biochemicals that include antibiotics, aflatoxins, and many other secondary products (*9–11*).

Very-long-chain PUFAs such as DHA and eicosapentaenoic acid (EPA, 20:5ω3) have been reported from several species of marine bacteria, including *Shewanella* sp. (*12–14*). Analysis of a genomic fragment (cloned as plasmid pEPA) from *Shewanella* sp. strain SCRC2738 identified five open reading frames (ORFs) that are necessary and sufficient for EPA production in *Escherichia coli* (*13*). Several of the predicted protein domains are homologs of FAS enzymes, and it was suggested that PUFA synthesis in *Shewanella* involved the elongation of 16- or 18-carbon fatty acids produced by FAS and the insertion of double bonds by undefined aerobic desaturases (*15*). We identified at least 11 regions within the five ORFs as putative enzyme domains (Fig. 1A). When compared with sequences in the nonredundant database (*16*), eight of these were more strongly related to PKS proteins than to FAS proteins (Fig. 1B). However, three regions were homologs of bacterial FAS proteins. One of these was similar to triclosan-resistant enoyl reductase (ER) from *Streptococcus pneumoniae* (*17*). Two regions were homologs of the *E. coli* FAS protein encoded by *fabA*, which catalyzes the synthesis of *trans*-2-decenoyl-ACP and the reversible isomerization of this product to *cis*-3-decenoyl-ACP (*18*). Thus, at least some of the double bonds in EPA from *Shewanella* are probably introduced by a dehydrase-isomerase mechanism catalyzed by the FabA-like domains in ORF7.

To exclude the involvement of an oxygen-

A

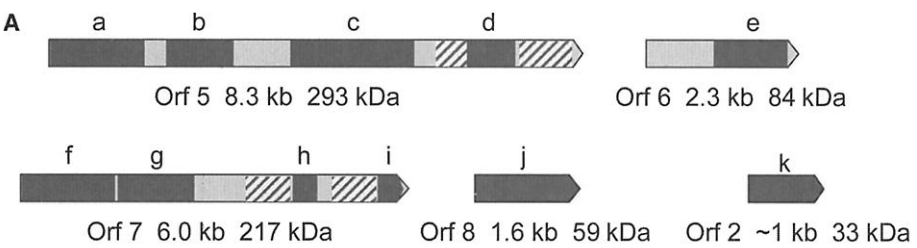

B

Domain	Approx. size (a.a)	Related to:	Putative function
a	490	PKS	3-ketoacyl synthase (KS); contains DXAC active site motif
b	350	PKS	malonyl-CoA:ACP acyltransferase (MAT)
c	640	PKS	acyl carrier protein (ACP); six repeats with LGXDS phosphopantetheine attachment site
d	250	PKS	3-ketoacyl-ACP reductase (KR)
e	400	PKS	acyl transferase (AT); contains GXSXG active-site motif
f	490	PKS	3-ketoacyl synthase (KS); contains DXAC active-site motif
g	400	PKS	chainlength factor (CLF), homologous to 3-ketoacyl synthase but no active-site C (*30*)
h, i	150	FAS	homologs of *E. coli* FabA dehydrase (DH)
j	540	FAS	homolog of *Streptococcus pneumoniae* enoyl reductase (ER)
k	300	PKS	phosphopantetheine transferase (*31*)

Fig. 1. Genomics analysis of *Shewanella* genes encoding enzymes of EPA synthesis. **(A)** Dark gray areas indicate proposed enzymatic domains. Hatched areas designate regions whose amino acid sequences are highly conserved amongst the EPA- and DHA-synthesizing proteins of *Shewanella*, *Moritella marina* (GenBank accession number AB025342.1), and *Schizochytrium* but for which potential enzymatic functions are not evident. Light gray indicates regions whose amino acid sequences are not conserved among these organisms. **(B)** Summary of sequence analysis data for the 11 domains designated a to k in (A) (*30*, *31*). a.a., amino acid.

[1]Omega Tech, 4909 Nautilus Court North, Boulder, CO 80301–3242, USA. [2]Monsanto, 1920 Fifth Street, Davis, CA 95616, USA. [3]Institute of Biological Chemistry, Washington State University, Pullman, WA 99164–6340, USA. [4]Sagami Chemical Research Center, 4–4–1 Nishi-Ohnuma, Sagamihara, Kanagawa 229, Japan.

*To whom correspondence should be addressed. E-mail: jmetz@omegadha.com (J.G.M.); jab@wsu.edu (J. B.)

†For the present addresses of these authors, contact J.G.M.

dependent desaturase in EPA synthesis, we cultured *E. coli* harboring the pEPA plasmid anaerobically. Anaerobically grown cells accumulated EPA to the same level as aerobic cultures (Fig. 2A). When pEPA was introduced into a *fabB*$^-$ mutant of *E. coli*, which is unable to synthesize unsaturated fatty acids that are required for growth, the resulting cells lost their fatty acid auxotrophy. They also accumulated higher concentrations of EPA than other pEPA-containing strains (Fig. 2A), suggesting that EPA competes with endogenously produced monounsaturated fatty acids for transfer to glycerolipids. Carbon–13 nuclear magnetic resonance (^{13}C-NMR) analysis of purified EPA from the cells grown in [^{13}C]acetate confirmed its structure and indicated that this fatty acid was synthesized from molecules derived from acetate (presumably acetyl-CoA and malonyl-CoA) (*19*). A cell-free homogenate from pEPA-containing *fabB*$^-$ cells synthesized both EPA and saturated fatty acids from [1-^{14}C]malonyl-CoA (Fig. 2B). High-speed centrifugation of the homogenate indicated that saturated fatty acid synthesis was confined to the supernatant, which is consistent with the soluble nature of the type II FAS enzymes (*20*). Synthesis of EPA was found only in the 200,000*g* pellet fraction, indicating that EPA synthesis does not rely on FAS or soluble intermediates (such as 16:0ACP) from the cytoplasmic fraction. Because the proteins encoded by the *Shewanella* genes are not particularly hydrophobic, restriction of EPA synthesis to this fraction may reflect a requirement for a membrane-associated acceptor molecule. In contrast to the *E. coli* FAS, EPA synthesis is specifically dependent on the reduced form of nicotinamide adenine dinucleotide phosphate (NADPH) and does not require NADH (Fig. 2C). These results are consistent with the pEPA genes encoding a multifunctional PKS that acts independently of FAS, elongase, and desaturase activities to synthesize EPA directly. Genes with homology to the *Shewanella* EPA gene cluster have been found in other PUFA-containing marine bacteria (*21*, *22*), indicating that the PKS pathway may be common in these organisms.

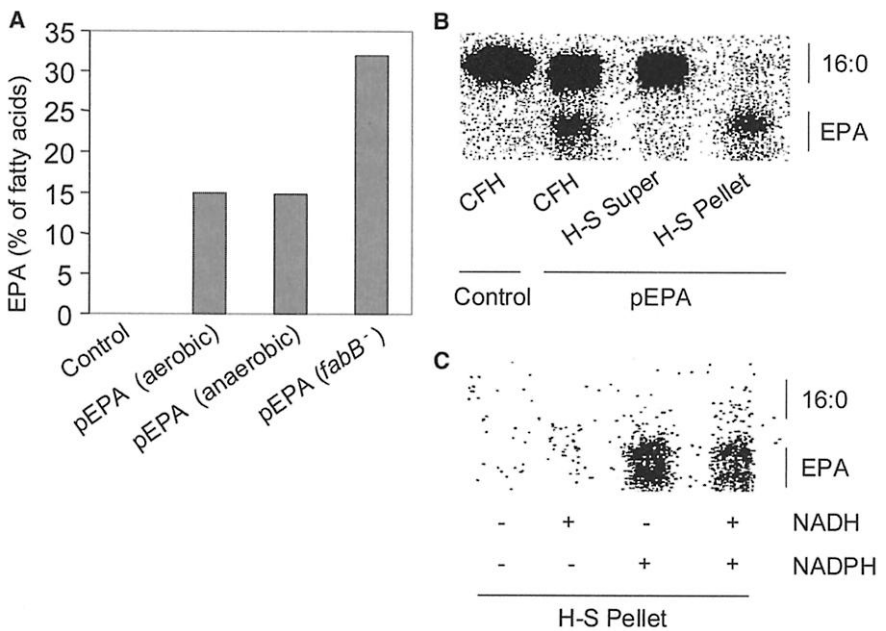

Fig. 2. Biochemical analysis of EPA synthesis in *E. coli*. (**A**) EPA accumulation in whole cells (quantified by gas chromatography analysis of methyl-ester derivatives) of *E. coli* containing a plasmid vector alone (control) or vector plus the *Shewanella* EPA genes [nucleotides 7708 to 35559 of GenBank accession number U73935.1 in the pNEB vector (New England BioLabs, Beverly, MA)]. Results were qualitatively similar with a variety of *E. coli* host strains; control cells never produced EPA, whereas the expression of the five EPA genes resulted in EPA accumulation. Cells were grown at 22°C (*13*) on media supplemented with glucose. EPA production in a *fadE*$^-$ mutant (deficient in fatty acid degradation) was compared when cells were grown under aerobic (pEPA-aerobic) and anaerobic (pEPA-anaerobic) growth conditions. Anaerobic conditions were achieved in Gas Pak Anaerobic Jars (Becton Dickinson Diagnostic Systems, Sparks, MD). The last column (pEPA-*fabB*$^-$) shows a level obtained when pEPA was expressed in the *fabB*$^-$ mutant. (**B**) Synthesis of EPA and saturated fatty acids from [1-^{14}C]malonyl-CoA in subcellular fractions from *fabB*$^-$ cells expressing the EPA genes. Control cells contained a vector alone and were maintained by the supplementation of growth medium with oleic acid. Cells were disrupted by passage through a French pressure cell and centrifuged (at 8000*g* for 10 min) to yield a cell-free homogenate (CFH). High-speed centrifugation (at 200,000*g* for 1 hour) was used to generate supernatant (H-S super) and membrane (H-S pellet) fractions. The H-S pellet was resuspended in buffer equivalent to the CFH volume. Aliquots were incubated in 50 mM phosphate buffer (pH 7.2), containing 20 μM acetyl-CoA, 100 μM [1-^{14}C]malonyl-CoA (0.9 GBq/mol), 2 mM dithiothreitol (DTT), 2 mM NADH, and 2 mM NADPH. Lipids were extracted and fatty acids were converted to methyl esters before separation by TLC (*19*). The figure shows radioactivity detected (with a radioanalytic scanner) on the TLC plate in the region in which saturated (16:0) and EPA methyl esters migrate. (**C**) Reductant requirement for in vitro EPA synthesis was tested with the H-S pellet fraction described in (B). Assays were carried out in reaction buffer containing 2 mM NADH and/or NADPH, or neither, as indicated. Incorporation of radioactivity into EPA was measured as described in (B).

Schizochytrium is a thraustochytrid marine protist that accumulates large quantities of triacylglycerols rich in DHA and docosapentaenoic acid (DPA, 22:5ω6) (*23*). In eukaryotes that synthesize 20- and 22-carbon PUFAs by an elongation-desaturation pathway, the pools of 18-, 20-, and 22-carbon intermediates are relatively large, so that in vivo labeling experiments with [^{14}C]acetate reveal clear precursor-product kinetics for the intermediates (*24*). In addition, radiolabeled intermediates provided exogenously to such organisms are converted to the final PUFA products (*25*). [1-^{14}C]acetate was rapidly taken up by *Schizochytrium* cells and incorporated into fatty acids (Fig. 3A). At 1 min, DHA contained 31% of the label recovered in fatty acids, and this percentage remained constant during the 10 to 15 min of [1-^{14}C]acetate incorporation and the subsequent 24 hours of culture growth. Similarly, DPA represented 10% of the label throughout the experiment. There is no evidence for a precursor-product relation between 16- or 18-carbon fatty acids and the 22-carbon polyunsaturated fatty acids (*25*). These results are consistent with rapid synthesis of DHA from [1-^{14}C]acetate involving very small (possibly enzyme-bound) pools of intermediates. A cell-free homogenate derived from *Schizochytrium* cultures incorporated [1-^{14}C]malonyl-CoA into DHA, DPA, and saturated fatty acids (Fig. 3C). The same biosynthetic activities were retained in a 100,000*g* supernatant fraction but were not present in the membrane pellet (Fig. 3C). Thus, DHA and DPA synthesis in *Schizochytrium* does not involve membrane-bound desaturases or fatty acid elongation enzymes such as those described for other eukaryotes (*7*, *8*). These fractionation data contrast with the data obtained from the *Shewanella* enzyme (Fig. 2B) and may indicate the use of a soluble acceptor molecule, such as CoA, by the *Schizochytrium* enzyme.

Additional support for a PKS-based pathway was provided from the sequencing of 8500 randomly selected clones from a *Schizochytrium* cDNA library (*26*). Within this data set, only one moderately expressed gene (0.3% of all sequences) was identified as a fatty acid desaturase, although a second putative desaturase was represented by a single clone (0.01%). In contrast, sequences that exhibited homology to 8 of the 11 domains of the *Shewanella* PKS genes (Fig. 1) were all identified at frequencies of 0.2 to 0.5%. Further sequencing of cDNA and genomic clones allowed the identification

of three ORFs containing domains with homology to those in *Shewanella* (Fig. 4). These proteins may constitute a PKS that catalyzes DHA and DPA synthesis. The homology between the prokaryotic *Shewanella* and eukaryotic *Schizochytrium* genes suggests that the PUFA PKS has undergone lateral gene transfer.

The primary structures of the *Shewanella* and *Schizochytrium* PKSs do not conform to any known class of PKS proteins (*9*, *10*). Instead, the data suggest that the PKSs synthesize PUFAs from malonyl-CoA (perhaps using acetyl-CoA as a primer) with an enzyme complex that carries out iterative processing of the fatty acyl chain but also performs trans-cis isomerization and enoyl reduction reactions in selected cycles. Although the exact sequence of reactions involved in PUFA synthesis remains to be determined, schemes can be envisioned that accommodate many aspects of the data (*27*).

The identification of the PUFA PKSs and of putative dehydrase-isomerases may provide new tools to engineer the production of additional polyketide antibiotics. In addition, characterization of PUFA synthesis in *Shewanella*, *Schizochytrium*, and their relatives has implications for understanding food web dynamics in aquatic ecosystems (*28*). Because these organisms are important primary producers of 20- and 22-carbon PUFAs in cold-water oceans (*12*), the PKS pathway may be a significant source of PUFAs for fish and mammals.

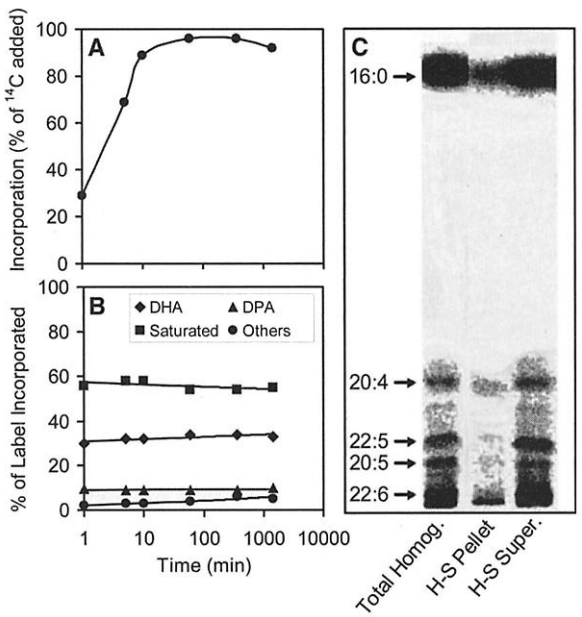

Fig. 3. Biochemical analysis of DHA synthesis in *Schizochytrium*. (A) and (B) In vivo labeling of *Schizochytrium* cells. [1-^{14}C]acetate was supplied to a 2-day-old culture as a single pulse at zero time. Samples of cells were then harvested by centrifugation and the lipids were extracted. (**A**) [1-^{14}C]acetate uptake by the cells was estimated by measuring the radioactivity of the sample before and after centrifugation. (**B**) Fatty acid methyl esters derived from the total cell lipids were separated by $AgNO_3$-TLC (solvent, hexane:diethyl ether: acetic acid, 70:30:2 by volume) (*32*). The identity of the fatty acid bands was verified by gas chromatography, and the radioactivity in them was measured by scintillation counting. (**C**) Synthesis of fatty acids from [1-^{14}C]malonyl-CoA in subcellular fractions from *Schizochytrium* cells. Cells were disrupted in 100 mM phosphate buffer (pH 7.2), containing 2 mM DTT, 2 mM EDTA, and 10% glycerol, by vortexing with glass beads. The cell-free homogenate was centrifuged at 100,000*g* for 1 hour. Equivalent aliquots of total homogenate, pellet (H-S pellet), and supernatant (H-S super) fractions were incubated in homogenization buffer supplemented with 20 μM acetyl-CoA, 100 μM [1-^{14}C]malonyl-CoA (0.9 GBq/mol), 2 mM NADH, and 2 mM NADPH for 60 min at 25°C. Assays were extracted and fatty acid methyl esters were prepared and separated as described above before detection of radioactivity with an Instantimager (Packard Instruments, Meriden, CT). The migration of fatty acid standards is indicated.

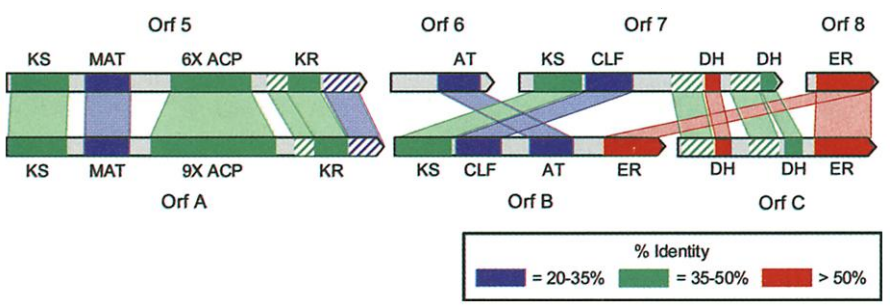

Fig. 4. Comparison of putative PKS enzyme domains in *Shewanella* and *Schizochytrium* ORFs (GenBank accession numbers: AF378327, AF378328, and AF378329). *Shewanella* domains were compared with the predicted *Schizochytrium* gene products by means of the LALIGN program (*29*) with matrix file BLOSUM50 and gap penalties of −14/−4 (opening/elongation). Boundaries and levels of protein sequence identity for regions identified by LALIGN are indicated. KS, 3-ketoacyl synthase; MAT, malonyl-CoA; ACP, acyl carrier protein; KR, 3-ketoacyl-ACP reductase; AT, acyl transferase; CLF, chainlength factor; ER, enoyl reductase; DH, dehydrase.

References and Notes

1. L. Lauritzen, H. S. Hansen, M. H. Jorgensen, K. F. Michaelsen, *Prog. Lipid Res.* **40**, 1 (2001).
2. M. McConn, J. Browse, *Plant J.* **15**, 521 (1998).
3. A. Heller, T. Koch, J. Schmeck, K. van Ackern, *Drugs* **55**, 487 (1998).
4. R. A. Creelman, J. E. Mullet, *Annu. Rev. Plant Physiol. Plant Mol. Biol.* **48**, 355 (1997).
5. The abbreviation *X:Y* indicates an acyl group containing *X* carbon atoms and *Y* cis double bonds; double-bond positions of PUFAs are indicated relative to the methyl carbon of the fatty acid chain (ω3 or ω6) with systematic methylene interruption of the double bonds.
6. H. Sprecher, *Curr. Opin. Clin. Nutr. Metab. Care* **2**, 135 (1999).
7. J. M. Parker-Barnes *et al.*, *Proc. Natl. Acad. Sci. U.S.A.* **97**, 8284 (2000).
8. J. Shanklin, E. B. Cahoon, *Annu. Rev. Plant Physiol. Plant Mol. Biol.* **49**, 611 (1998).
9. D. A. Hopwood, D. H. Sherman, *Annu. Rev. Genet.* **24**, 37 (1990).
10. R. Bentley, J. W. Bennett, *Annu. Rev. Microbiol.* **53**, 411 (1999).
11. T. A. Keating, C. T. Walsh, *Curr. Opin. Chem. Biol.* **3**, 598 (1999).
12. D. Nichols *et al.*, *Curr. Opin. Biotechnol.* **10**, 240 (1999).
13. K. Yazawa, *Lipids* **31**, S-297 (1996).
14. F. DeLong, A. A. Yayanos, *Appl. Environ. Microbiol.* **51**, 730 (1986).
15. K. Watanabe, K. Yazawa, K. Kondo, A. Kawaguchi, *J. Biochem.* **122**, 467 (1997).
16. S. F. Altschul *et al.*, *Nucleic Acids Res.* **25**, 3389 (1997). Gapped BLAST and PSI-BLAST protein database search software is available at http://www.ncbi.nlm.nih.gov/.
17. R. J. Heath, C. O. Rock, *Nature* **406**, 145 (2000). Comparison of ORF8 peptide with the *S. pneumoniae* ER with the LALIGN program (*29*) (matrix, BLOSUM50; gap opening penalty, −10; gap elongation penalty, −1) indicated 49% similarity over a 386–amino acid overlap.
18. R. J. Heath, C. O. Rock, *J. Biol. Chem.* **271**, 27795 (1996).
19. *E. coli* (FadE$^-$) cells containing the pEPA plasmid were grown to an optical density at 600 nm (OD_{600}) of ~1 at 21°C in 250 ml of liquid medium supplemented with 100 mg of either [1-^{13}C]- or [2-^{13}C]sodium acetate. Cells were collected and lipids extracted with chloroform and methanol (at a ratio of 2:1, v/v). Fatty acid methyl esters were produced by using 0.4 ml of 9% sulfuric acid in methanol and 0.2 ml of toluene at 90°C for 1 hour. EPA-methyl esters were purified by thin-layer chromatography (TLC) [silica gel G glass plates were migrated three times in hexane and diethyl ether (95:5, v/v)], scraped from the plates, and eluted with deuterated chloroform. ^{13}C-NMR spectra of the samples were obtained on a General Electric NMR OMEGA 500 mHz instrument, and these spectra confirmed the identity of the EPA as 20:5ω3. The label from [1-^{13}C]acetate was incorporated into odd-numbered carbons, whereas the label from [2-^{13}C]acetate was incorporated into even-numbered carbons.
20. K. Magnuson, S. Jackowski, C. O. Rock, J. E. Cronan Jr., *Microbiol. Rev.* **57**, 522 (1993).
21. E. E. Allen, D. Facciotti, D. H. Bartlett, *Appl. Environ. Microbiol.* **65**, 1710 (1999).
22. M. Tanaka *et al.*, *Biotechnol. Lett.* **21**, 939 (1999).
23. W. R. Barclay, K. M. Meager, J. R. Abril, *J. Appl. Phycol.* **6**, 123 (1994).
24. J. L. Gellerman, H. Schlenk, *Biochim. Biophys. Acta* **573**, 23 (1979).
25. We also supplied *Schizochytrium* cultures with ^{14}C-labeled 16:0, 18:1, or 18:3 fatty acids (as the sodium salts). Over 90% of the label was incorporated into triacylglycerols and phospholipids, and 10 min after

the addition of substrate, less than 5% of the radioactivity remained as unesterified fatty acid. These results indicate that the fatty acids were taken up by the cells and used in the cellular reactions of lipid synthesis. However, 24 hours after the start of the experiments, 96 to 98% of the radioactivity was recovered as the original fatty acid supplied and no label could be detected in DHA or DPA.

26. mRNA was isolated from PUFA-producing *Schizochytrium* (American Type Culture Collection number 20888) cells grown in a fermentor, and a cDNA library was produced with the GIBCO BRL Superscript Plasmid Cloning System with vector pSPORT1. Clones were randomly chosen and sequenced from the 5′ end with a universal sequencing primer.
27. Supplementary material is available on *Science* Online at www.sciencemag.org/cgi/content/full/293/5528/290/DC1. Included is a description of one possible reaction scheme. A key feature of this and similar schemes is the incorporation of the cis double bonds during fatty acyl chain formation by the action of the FabA dehydrase/isomerase domains.
28. D. C. Muller-Navarra, M. T. Brett, A. M. Liston, C. R. Goldman, *Nature* **403**, 74 (2000).
29. W. R. Pearson, *Methods Mol. Biol.* **132**, 185 (2000).
30. C. Bisang *et al.*, *Nature* **401**, 502 (1999).
31. We indicate the size of ORF2 as ~1.0 kb in contrast to the 0.83 kb given in the GenBank accession number U73935.1. Expression of ORF2 in *E. coli* with the ATG at position 9016 as the start codon did not produce a functional protein. In contrast, a clone including the TTG codon at position 9157 did result in production of a functional protein. Several other potential bacterial start codons (i.e., TTG or ATT) are present between positions 9157 and 9016, and it is possible that one of these codons may represent the actual start codon in *Shewanella*.
32. M. Miquel, J. Browse, *J. Biol. Chem.* **267**, 1502 (1992).
33. We thank J. Cronan (Univ. of Illinois) for the gift of *E. coli* strains, B. Shen (Univ. of CA Davis) for the help with NMR analyses, and J. Kuner (OmegaTech, Boulder, CO) for assistance with *Schizochytrium* gene sequencing. Supported in part by grants from Monsanto and the U.S. Department of Energy (grant DE-FG03-99ER20323) to J.B. and by the Agricultural Research Center, Washington State University, Pullman, WA.

5 February 2001; accepted 1 June 2001

Endothelial Apoptosis as the Primary Lesion Initiating Intestinal Radiation Damage in Mice

François Paris,[1] Zvi Fuks,[2] Anthony Kang,[1] Paola Capodieci,[3] Gloria Juan,[3] Desiree Ehleiter,[1] Adriana Haimovitz-Friedman,[2] Carlos Cordon-Cardo,[3] Richard Kolesnick[1]*

Gastrointestinal (GI) tract damage by chemotherapy or radiation limits their efficacy in cancer treatment. Radiation has been postulated to target epithelial stem cells within the crypts of Lieberkühn to initiate the lethal GI syndrome. Here, we show in mouse models that microvascular endothelial apoptosis is the primary lesion leading to stem cell dysfunction. Radiation-induced crypt damage, organ failure, and death from the GI syndrome were prevented when endothelial apoptosis was inhibited pharmacologically by intravenous basic fibroblast growth factor (bFGF) or genetically by deletion of the acid sphingomyelinase gene. Endothelial, but not crypt, cells express FGF receptor transcripts, suggesting that the endothelial lesion occurs before crypt stem cell damage in the evolution of the GI syndrome. This study provides a basis for new approaches to prevent radiation damage to the bowel.

The GI syndrome is the main toxicity associated with abdominal radiotherapy of human tumors. It consists of diarrhea, dehydration, enterobacterial infection, and in severe cases, septic shock and death (*1*). According to the prevailing hypothesis, it is caused by direct damage to a group of stem cells within the epithelial rings at positions 4 to 5 from the base of the crypts of Lieberkühn, resulting in their death (*1–3*). This etiological model is based on inference from studies of crypt regeneration after injury by using an in vivo clonogenic survival assay. Stem cell death is the critical element in the evolution of this process, because a single surviving stem cell appears sufficient for reconstitution of a crypt-villus unit (*1*). This clonogenic stem cell activity is quantified by counting regenerating crypts in histologic sections 3.5 days after irradiation (*1*). Above 8 grays (Gy), dose-dependent stem cell death leads to diminution of crypt regeneration, until the level of regeneration is insufficient to rescue the GI mucosa. In such cases, progressive denudation of the epithelium leads, by day 6 to 7 after radiation, to death of mice from the GI syndrome. Direct evaluation of stem cell function in this process is, however, not feasible because there are no markers specific for GI stem cells.

Here, we explore the alternative possibility that microvascular endothelium within the intestinal mucosa is the actual target of radiation damage, with stem cell dysfunction as a consequence. This hypothesis is supported by previous observations that (i) survival factors for endothelium [vascular endothelial growth factor (VEGF), acidic and basic FGFs, and interleukin 11 (IL-11)] protect the gut from radiation injury (*4–6*), and (ii) endothelium is a principal target for radiation injury to lung and brain (*7, 8*).

In our initial studies, we used a murine whole-body irradiation (WBR) model (*9*). The patterns of lethality and tissue damage are shown (Fig. 1) for 8- to 12-week-old C57BL/6 mice exposed to 12 to 15 Gy WBR, which exceeds the minimal dose required to kill all exposed animals within 30 days ($LD_{100/30}$). When treated with 12 or 13 Gy, 97% of mice died 10 to 13 days after irradiation (median 11 days; Fig. 1A) and displayed bone marrow aplasia and intact intestinal mucosa (Fig. 1B). Autologous marrow transplantation, performed 16 hours after 12 Gy WBR, repopulated the marrow (*10*) and rescued 90% of the mice. In contrast, exposure to 15 Gy resulted in more rapid death, with 95% of the mice dying between 6 and 8 days (mean 6.8 ± 0.99 days, median 6 days; Fig. 1A). These animals showed denudation of the intestinal crypt and villus system but had only partially damaged marrow (Fig. 1B), and could not be rescued by autologous marrow transplantation (Fig. 1A). Actuarial survival at 14 Gy differed significantly from that after 15 Gy ($P < 0.001$). At this dose, 25% of mice succumbed to death from the GI syndrome and 75% died of marrow failure ($P = 0.007$ versus death from GI syndrome at 15 Gy).

To determine whether microvascular endothelial apoptosis correlated with development of the radiation-induced GI syndrome, we evaluated tissue specimens by hematoxylin and eosin (H&E) staining, terminal dexoy transferase-mediated deoxyuridine triphosphate nick end labeling (TUNEL), and in situ labeling with annexin V (*11*), at various times after 8 to 15 Gy WBR. Previous studies have shown that radiation induces early p53-dependent (*12*) and late p53-independent (*13*) apoptotic responses in crypt epithelial cells. However, neither response affects the ability of stem cells to regenerate crypts damaged by doses ≤15 Gy (*13*) and hence do not appear to be involved in the pathogenesis of the GI syndrome. Using a published scoring system (*14*), we confirmed these observations and found a maximal epithelial apoptotic index of 40.0% at crypt position at 4 hours after 15 Gy, which decreased to 24.1% at position 5 and progressively to 4.1% at position 8. The apopto-

[1]Laboratory of Signal Transduction and [2]Department of Radiation Oncology and [3]Department of Pathology, Memorial Sloan-Kettering Cancer Center, 1275 York Avenue, New York, NY 10021, USA.

*To whom correspondence should be addressed. E-mail: r-kolesnick@ski.mskcc.org